Table 1. Association between polymorphisms in LID with rs3739708 and knee OA

Polymorphism ID (i-*EDG2*-x)	Genotype[a] Case				Control				11 frequency (%) Case	Control	*P*-value Allele	11 versus	22 versus
	11	12	22	Sum	11	12	22	Sum					
1	0	31	613	644	0	26	613	639	0	0	0.5	–	0.5
2	0	83	561	644	4	74	562	640	0	0.6	1	0.04	0.7
3	57	254	333	644	29	252	359	640	8.9	4.5	0.01	0.002	0.1
4	9	154	481	644	12	159	466	637	1.4	1.9	0.5	0.5	0.5
5	0	84	560	644	4	74	560	638	0	0.6	0.9	0.04	0.7
6	0	19	622	641	0	29	608	637	0	0	0.1	–	0.1
7	9	152	482	643	10	150	472	632	1.4	1.6	0.9	0.8	0.9
8	155	329	159	643	135	310	193	638	24.1	21.2	0.03	0.2	0.03
9	64	255	325	644	33	251	356	640	9.9	5.2	0.005	0.001	0.1
10	0	37	606	643	3	30	604	637	0	0.5	0.9	0.1	0.7
11	0	86	558	644	5	77	556	638	0	0.8	0.9	0.02	0.8
12	74	266	304	644	38	275	327	640	11.5	5.9	0.009	0.0004	0.2
13	0	86	556	642	6	77	557	640	0	0.9	0.8	0.01	0.8
14	0	87	557	644	4	78	556	638	0	0.6	1	0.04	0.7
15	151	326	166	643	140	316	182	638	23.5	21.9	0.3	0.5	0.3
16	154	329	160	643	133	311	194	638	24	20.8	0.03	0.2	0.03
17	0	84	559	643	4	78	556	638	0	0.6	0.8	0.04	0.9
18	48	225	371	644	30	221	387	638	7.5	4.7	0.08	0.04	0.3
19	119	315	209	643	106	282	250	638	18.5	16.6	0.03	0.4	0.01
20	1	13	629	643	0	16	622	638	0.2	0	0.8	0.3	0.7
21	0	86	558	644	4	80	556	640	0	0.6	0.8	0.04	0.9
22	9	152	483	644	10	152	476	638	1.4	1.6	0.8	0.8	0.9
23	0	64	580	644	2	69	567	638	0	0.3	0.4	0.2	0.5
24	111	327	206	644	99	302	236	637	17.2	15.5	0.08	0.4	0.1
25[b]	45	225	373	643	22	212	404	638	7	3.4	0.007	0.004	0.1
26	0	66	578	644	2	69	567	638	0	0.3	0.5	0.2	0.6
27	2	36	604	642	3	55	578	636	0.3	0.5	0.03	0.6	0.03

[a]11, 12 and 22 indicate homozygotic for the minor allele, and heterozygotic and homozygotic for the major allele, respectively.
[b]Landmark SNP.

reporter gene. As an inducer of AP-1, we used phorbol myristate acetate (PMA), which is known to increase AP-1-binding activity in synovial cells (10). PMA stimulation increased luciferase activity, which was higher in cells transfected with the vector harboring the susceptibility A allele (Fig. 1A).

We then examined the allelic difference in the binding of i-*EDG2*-9 to *trans* factors by electrophoretic mobility shift assay (EMSA). PMA stimulation increased AP-1 transcriptional activity in E11 cells in a dose-dependent manner (Supplementary Material, Fig. S3). Nuclear extracts from E11 cells stimulated by PMA formed DNA–protein complexes with oligonucleotides harboring i-*EDG2*-9 in a time-dependent manner (Fig. 1B). The band intensity for DNA–protein complexes derived from the A allele was higher than that from the G allele (Fig. 1C). The complex was diminished by excess amounts of a non-labeled oligonucleotide with the AP-1 consensus sequence. These data suggest that the *EDG2* promoter harboring the A allele tends to express higher levels of *EDG2* transcripts owing to a stronger binding affinity for AP-1.

The role of LPA/EDG2 system in synovium

To examine the role of LPA/EDG2 signaling in synovium, we stimulated primary fibroblast-like cells derived from the inflamed synovial tissue of an OA patient (HFLS-OA) by LPA and examined the gene expression of inflammatory cytokines and MMPs involved in the catabolic process of OA (11). LPA stimulation resulted in an early and transient expression increase of the inflammatory cytokine genes for interleukin-1β (IL-1β), tumor necrosis factor-α (TNF-α), and IL-6 (Fig. 2A–C), as well as upregulation of MMP genes (Fig. 2D–F). LPA treatment induced the inflammatory cytokine genes in a dose-dependent manner (Fig. 2G–I). The induction was inhibited by treatment with a pharmacological EDG2 antagonist, Ki16425 (Fig. 2J), and by introducing siRNA targeting *EDG2* into HFLS-OA (Fig. 2K, L). These findings indicate that *EDG2* is critical for the catabolic response in synovial tissue caused by LPA signaling.

DISCUSSION

We have shown that a functional SNP in the *EDG2* region is associated with knee OA. We have further demonstrated that this SNP affects AP-1-mediated transcriptional activity, which may result in increased *EDG2* expression when the allele is over-represented in knee OA patients. Expressional and functional analyses revealed that EDG2 is the critical LPA receptor in synovium. OA is not just a cartilage disease, but also affects the entire joint structure including the synovial membrane, subchondral bone and ligament (12). To our knowledge, however, *EDG2* is the first OA-related gene to be primarily expressed in the synovium, highlighting the importance of the synovium in the pathogenesis of OA.

In the OA synovium, inflammatory changes occur including synovial hypertrophy and hyperplasia with an increased

Table 2. Association test in resident-cohort population

Polymorphism ID (i-*EDG2*-x)	Genotype[a] Case				Control				11 frequency (%) Case	Control	*P*-value[b]	Odds ratio[b] (95% CI)
	11	12	22	Sum	11	12	22	Sum				
3	14	81	143	238	8	103	163	274	5.9	2.9	0.099	2.08 (0.86–5.05)
9	18	78	142	238	6	101	172	279	7.6	2.2	0.0036	3.72 (1.45–9.53)
12	17	86	135	238	6	108	165	279	7.1	2.2	0.0061	3.50 (1.36–9.03)
25[c]	12	72	154	238	5	88	185	278	5	1.8	0.04	2.9 (1.01–8.35)

[a]11, 12 and 22 indicate homozygotic for the minor allele, and heterozygotic and homozygotic for the major allele, respectively.
[b]*P*-value and odds ratio were calculated using the recessive model.
[c]i-*EDG2*-25 is identical to rs3739708, the landmark SNP.

number of lining cells (13). Also, the production of inflammatory cytokines such as IL-1β, TNF-α and cartilage-degradating enzymes such as the MMPs is enhanced (14,15). Inflammatory cytokines and MMPs released from the synovium affect the articular cartilage in a paracrine manner via the synovial fluid, and they promote a catabolic process that leads to progressive cartilage degradation. We have shown here that LPA induces both inflammatory cytokines and MMPs in synovial fibroblasts via EDG2, suggesting that LPA/EDG2 signaling is involved in the pathogenesis of OA via this catabolic process. Our findings could therefore provide new therapeutic options for OA using druggable targets.

MATERIALS AND METHODS

Selection of SNPs

We selected 64 GPCRs expressed in the cartilage based on GeneChip (Affymetrix) analysis using total cartilage RNAs from eight OA and eight normal individuals described previously (16). We excluded one gene located on the X chromosome from further study. Next, we estimated haplotype-tagging of SNPs for the 63 cartilage GPCR genes located on autosomal chromosomes using large-scale genotype data described elsewhere (17). We excluded genes not having any Invader probe labeling or showing a minor allele frequency of no >10%. We determined the haplotype block structure of each gene by a method reported by Gabriel *et al.* (18), and selected SNPs that represented any haplotype having a frequency >0.1% in each haplotype block. Finally, we selected 167 SNPs for 44 genes (Supplementary Material, Table S1).

SNP discovery and genotyping

For a fine-scale association study and LD mapping of the 45 kb region containing exon 1 of *EDG2*, we detected SNPs by direct sequencing of genomic DNA from 48 affected individuals as described previously (19,20). We genotyped the SNPs using the Invader assay, TaqMan assay, and direct sequencing of PCR products with capillary sequencers (ABI3700, Applied biosystems), and we then tested for association.

Subjects

All individuals recruited for this study were Japanese and received clinical and radiographic examination by orthopedic specialists. The selection method and criteria were described previously (16). We recruited case–control subjects from individuals who lived in mainland Japan (Honshu), and visited the participating clinical institutions. We studied 644 individuals with knee OA (83% female; mean age ± SD = 71.7 ± 7.7 years) and 640 controls (36% female; mean age ± SD = 61.5 ± 10.3 years). In the second screen of the stepwise screening, we used genotype data of another 654 controls from a previous study (45% female; mean age ± SD = 48.5 ± 21.6 years) (17). The minor allele's homozygote frequencies for the landmark SNP (rs3739708) in these two controls were almost the same (3.4 and 3.5%, respectively). All affected individuals were symptomatic and were treated in the participating institutions on a regular basis.

We also recruited resident-cohorts from inhabitants of Miyagawa village and Nansei town in Mie prefecture, which is located in the middle of mainland Japan. For each individual, we took standard three-direction knee radiographs. Using the KL grade and self-reported pain, we classified Miyagawa village subjects into OA (KL grade 2–4) and non-OA (KL grade 0–1 and without self-reported pain) groups. We also classified Nansei town subjects into OA (JSN grade 2–5) and non-OA (JSN grade 1 and without self-reported pain) groups. The OA group consisted of 238 subjects (75% female; mean age ± SD = 71.5 ± 7.8 years) and the non-OA group consisted of 279 subjects (62% female; mean age ± SD = 68.8 ± 8.1 years). Other clinical parameters were described previously (16).

The study protocol was approved by the ethical committees of the SNP Research Center of RIKEN and the participating institutions, and written informed consent was obtained from each participant. We obtained blood samples from the participants and prepared genomic DNA from peripheral leukocytes in accordance with standard protocols.

Association analysis

We used case–control subjects for a stepwise association study and genotyped 167 SNPs in genomic DNA from 368 individuals with knee OA and 323 control individuals. For the successfully genotyped SNPs, which were in Hardy–Weinberg equilibrium in the control population, we calculated

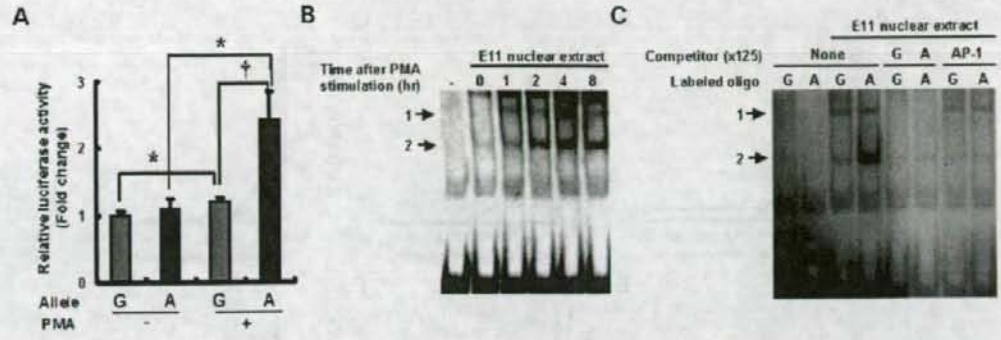

Figure 1. Transcriptional regulatory activity is affected by i-*EDG2*-9. (**A**) Luciferase promoter assay. Allelic differences in the relative luciferase activity were compared with or without 10 ng/ml of PMA. The promoter containing the susceptibility A allele showed significantly stronger activity upon PMA stimulation. Data show the mean ± SEM of values from four transfections. Asterisk and dagger indicate $P < 0.05$ and 0.01 by Student's *t*-test, respectively. (**B**, **C**) EMSA. (B) Binding of i-*EDG2*-9 to components of nuclear extracts from E11 cells stimulated by PMA. Band 2 showed increased binding in a time-dependent manner. Band 1 did not change in intensity over the course of the experiment. (C) Allelic difference in binding. Band 2 indicates tighter binding of the oligonucleotide containing the A allele compared with that containing the G allele. This binding was blocked by addition of a 125-fold excess of unlabeled oligonucleotides as well as an oligonucleotide with the AP-1 binding motif. Band 1 did not show allelic difference or competition by the unlabeled oligonucleotide with AP-1 binding motif. The experiment was repeated three times with similar results.

P-values as previously described (the first screen) (21). SNPs that passed the first screen were further genotyped in a second replication panel consisting of 276 individuals with knee OA and the association was tested using control genotype data of 654 individuals that were genotyped in a previously study (17) as an independent test (the second screen). For both screens, *P*-values <0.05 were considered significant.

After identification of the landmark SNP through the stepwise screening followed by LD mapping and re-sequence of the LD region containing the SNP (rs3739708), all discovered SNPs within the region were genotyped for a total of 644 OA cases (all the cases of the first and second screens) and 640 controls (323 controls of the first screen and 317 controls further recruited). Then, we calculated the final *P*-value of the case–control population using the genotype data.

Human articular cartilage and synovium samples

We obtained cartilage and synovium from individuals with knee OA during surgery (total knee arthroplasty). These samples were immediately frozen in liquid nitrogen and stored at −80 °C.

Statistical analysis

We carried out statistical analysis for the association study, Hardy–Weinberg equilibrium, calculation of LD coefficients (D') and LD index (Δ) as described previously (21,22). We estimated haplotype frequencies using the expectation–maximization algorithm (23). We performed a Mantel–Haenszel analysis to calculate the pooled *P*-value and odds ratio of two independent association studies (case–control and resident-cohort). Luciferase assay data were analyzed by Student's *t*-test using Excel software (Microsoft).

Cell culture

HFLS-OA, primary fibroblast-like cells derived from the inflamed synovial tissue of an OA patient, was purchased from Cell Applications. HFLS-OA was routinely cultured in synoviocyte growth medium (Cell Applications). We used these cells within five passages. For the gene expression assay, cells were plated on a 24-well plate at 1×10^5 cells/well in synoviocyte growth medium. After reaching confluence, cells were cultured in Ham's F-12 medium (Invitrogen) containing 0.1% fatty acid-free BSA (Bovine serum albumin, Sigma) for 12 h, and then stimulated by LPA (1-oleyl-*sn*-glycerol-3-phosphate, Sigma) with or without an LPA1/3 antagonist Ki16425 (Sigma).

For the luciferase assay and EMSA, we used E11, a fibroblast-like synovial cell line (9). We grew E11 cells in Dulbecco's Modified Eagle's medium (Sigma) supplemented with 10% FBS (Fetal bovine serum) containing 2 mM L-glutamine and antibiotics (100 U/ml penicillin-G and 100 μg/ml streptomycin).

siRNA

The siRNA directed against human *EDG2* was designed using the siRNA design support system in the Takara Bio website (http://www.takara-bio.co.jp). As a control, we used a scrambled siRNA targeted against asporin as described elsewhere (24). The siRNA and control were synthesized by Takara Bio. Oligonucleotide sequences are listed in Supplementary Material, Table S6. We transfected siRNAs into HFLS-OA cells using TransIT TKO (Mirus), and cultured the cells for 36 h in complete synoviocyte growth medium. We cultured the cells in Ham's F-12 medium containing 0.1% fatty acid-free BSA for a further 12 h, and then the stimulated cells by application of 10 μM LPA for 2 h.

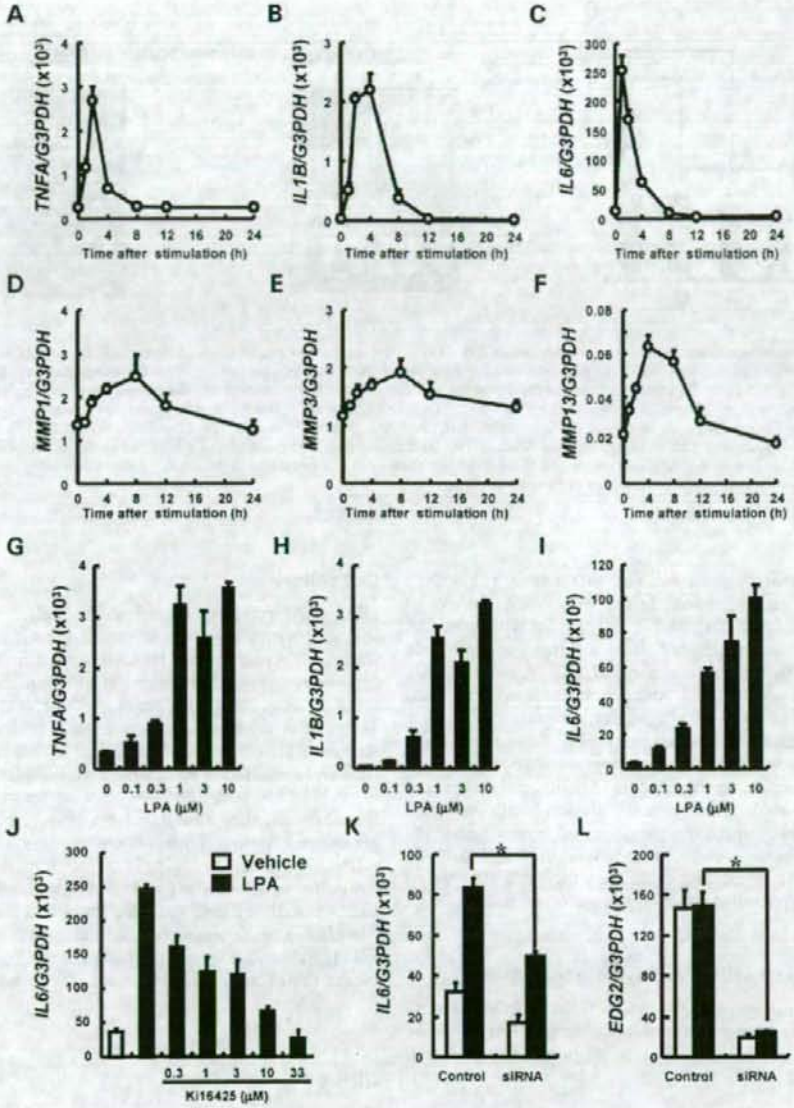

Figure 2. Induction of pro-inflammatory cytokines and MMPs by LPA. Real-time PCR in a human synovial cell line, HFLS-OA. (**A**–**F**) Time course of induction by 10 mM LPA for pro-inflammatory cytokine genes (A) *TNFA*, (B) *IL1B* and (C) *IL6* and MMP genes (D) *MMP1*, (E) *MMP3* and (F) *MMP13*. (**G**–**I**) Dose-dependent induction by LPA of pro-inflammatory cytokine genes (G) *TNFA*, (H) *IL1B* and (I) *IL6*. (**J**–**L**) Inhibition of LPA-induced *IL6* expression by an antagonist, Ki16425 (J) and siRNA (K) targeting *EDG2* in HFLS-OA cells. Decreased expression of *EDG2* was confirmed (L). Data show the mean ± SEM of triplicate or quadruplicate assay.

Real-time PCR

We extracted total RNA from clinical samples or cells using Isogen (Nippongene) and purified them using an SV-Total RNA Isolation system (Promega). We synthesized first-strand cDNA. We carried out real-time PCR on an ABI PRISM 7700 sequence detection system (Applied biosystems) using QuantiTect SYBR Green PCR (Qiagen) according to the manufacturer's instructions. First-strand cDNA was amplified using primers specific for LPA receptor genes (*EDG2*, *EDG4*, *EDG7* and *GPR23*) or pro-inflammatory cytokine genes (*TNFA*, *IL1B* and *IL6*) and *G3PDH* (Toyobo). The expression

of LPA receptor genes and pro-inflammatory cytokine genes was normalized to that of *G3PDH* from the same cDNA using a standard curve method described by the manufacturer. Specific primer sequences are listed in Supplementary Material, Table S7.

Electrophoretic mobility shift assay

We grew E11 cells until confluency and then cultured them with 10 ng/ml PMA (Sigma) for 0–8 h. We prepared a nuclear extract from these cells as previously described (25). We incubated the nuclear extract with 36 bp double-strand oligonucleotide probes for i-*EDG2*-9 alleles (G and A) for 20 min at room temperature. Oligonucleotide sequences are listed in Supplementary Material, Table S6. The AP-1 oligonucleotide sequence was described elsewhere (26). Probes were labeled using the digoxigenin gel-shift kit (Roche). For competition studies, we pre-incubated the nuclear extract with unlabeled oligonucleotides (125-fold excess) before adding the labeled oligonucleotide. Protein–DNA complexes were separated by electrophoresis on a 6% polyacrylamide gel in 0.5× TBE (Tris-borate-EDTA) buffer, followed by transfer to a nitrocellulose membrane and detection using a chemiluminescent signal detection system (Roche).

Luciferase assay

We constructed a luciferase reporter plasmid by cloning five connected copies of the adjacent 36 bp double-strand oligonucleotides containing the i-*EDG2*-9 allele into the pGL3-promoter vector (Promega) upstream of the SV40 promoter as described previously (27). We transfected E11 cells (5×10^4 cells/well) with 0.2 μg of the constructs and 4 ng of pRL-TK vector (Promega) as an internal control for transfection efficiency using Fugene-6 (Roche). After 24 h, we cultured the transfected cells with or without 10 ng/ml of PMA. After 5 h, cells were solubilized and luciferase activity was measured using the Pikkagene dual luciferase assay system (Toyo Ink, Tokyo, Japan).

Accession numbers

Human *EDG2* mRNA, NM_057159.

SUPPLEMENTARY MATERIAL

Supplementary Material is available at HMG Online.

ACKNOWLEDGEMENTS

We thank patients for participating in the study. We also thank Dr. Seizo Yamamoto for help in performing the study, and Ms. Tomoko Kusadokoro for excellent technical assistance.

Conflict of Interest statement. None declared.

REFERENCES

1. Oliveria, S.A., Felson, D.T., Reed, J.I., Cirillo, P.A. and Walker, A.M. (1995) Incidence of symptomatic hand, hip, and knee osteoarthritis among patients in a health maintenance organization. *Arthritis Rheum.*, **38**, 1134–1141.
2. Felson, D.T. and Zhang, Y. (1998) An update on the epidemiology of knee and hip osteoarthritis with a view to prevention. *Arthritis Rheum.*, **41**, 1343–1355.
3. Wieland, H.A., Michaelis, M., Kirschbaum, B.J. and Rudolphi, K.A. (2005) Osteoarthritis—an untreatable disease? *Nat. Rev. Drug Discov.*, **4**, 331–344.
4. Stecher, R.M. (1941) Heberden's nodes: heredity in hypertrophic arthritis of the finger joints. *Am. J. Med. Sci.*, **201**, 801–809.
5. Spector, T.D., Cicuttini, F., Baker, J., Loughlin, J. and Hart, D. (1996) Genetic influences on osteoarthritis in women: a twin study. *BMJ*, **312**, 940–943.
6. Ikegawa, S. (2007) New gene associations in osteoarthritis: what do they provide, and where are we going? *Curr. Opin. Rheumatol.*, **19**, 429–434.
7. Hopkins, A.L. and Groom, C.R. (2002) The druggable genome. *Nat. Rev. Drug Discov.*, **1**, 727–730.
8. Ishii, I., Fukushima, N., Ye, X. and Chun, J. (2004) Lysophospholipid receptors: signaling and biology. *Annu. Rev. Biochem.*, **73**, 321–354.
9. Mori, N., Murakami, S., Oda, S., Prager, D. and Eto, S. (1995) Production of interleukin 8 in adult T-cell leukemia cells: possible transactivation of the interleukin 8 gene by human T-cell leukemia virus type I tax. *Cancer Res.*, **55**, 3592–3597.
10. Lin, C.W., Robbins, P.D., Georgescu, H.I. and Evans, C.H. (1996) Effects of immortalization upon the induction of matrix metalloproteinases in rabbit synovial fibroblasts. *Exp. Cell Res.*, **223**, 117–126.
11. Smith, G.N., Jr (2006) The role of collagenolytic matrix metalloproteinases in the loss of articular cartilage in osteoarthritis. *Front. Biosci.*, **11**, 3081–3095.
12. Felson, D.T., Lawrence, R.C., Dieppe, P.A., Hirsch, R., Helmick, C.G., Jordan, J.M., Kington, R.S., Lane, N.E., Nevitt, M.C., Zhang, Y. *et al.* (2000) Osteoarthritis: new insights. *Ann. Intern. Med.*, **133**, 635–646.
13. Pelletier, J.P., Martel-Pelletier, J. and Abramson, S.B. (2001) Osteoarthritis, an inflammatory disease: potential implication for the selection of new therapeutic targets. *Arthritis Rheum.*, **44**, 1237–1247.
14. Smith, M.D., Triantafillou, S., Parker, A., Youssef, P.P. and Coleman, M. (1997) Synovial membrane inflammation and cytokine production in patients with early osteoarthritis. *J. Rheumatol.*, **24**, 365–371.
15. Lark, M.W., Bayne, E.K., Flanagan, J., Harper, C.F., Hoerner, L.A., Hutchinson, N.I., Singer, I.I., Donatelli, S.A., Weidner, J.R., Williams, H.R. *et al.* (1997) Aggrecan degradation in human cartilage. Evidence for both matrix metalloproteinase and aggrecanase activity in normal, osteoarthritic, and rheumatoid joints. *J. Clin. Invest.*, **100**, 93–106.
16. Kizawa, H., Kou, I., Iida, A., Sudo, A., Miyamoto, Y., Fukuda, A., Mabuchi, A., Kotani, A., Kawakami, A., Yamamoto, S. *et al.* (2005) An aspartic acid repeat polymorphism in asporin inhibits chondrogenesis and increases susceptibility to osteoarthritis. *Nat. Genet.*, **37**, 138–144.
17. Mototani, H., Mabuchi, A., Saito, S., Fujioka, M., Iida, A., Takatori, Y., Kotani, A., Kubo, T., Nakamura, K., Sekine, A. *et al.* (2005) A functional single nucleotide polymorphism in the core promoter region of *CALM1* is associated with hip osteoarthritis in Japanese. *Hum. Mol. Genet.*, **14**, 1009–1017.
18. Gabriel, S.B., Schaffner, S.F., Nguyen, H., Moore, J.M., Roy, J., Blumenstiel, B., Higgins, J., DeFelice, M., Lochner, A., Faggart, M. *et al.* (2002) The structure of haplotype blocks in the human genome. *Science*, **296**, 2225–2229.
19. Ozaki, K., Ohnishi, Y., Iida, A., Sekine, A., Yamada, R., Tsunoda, T., Sato, H., Sato, H., Hori, M., Nakamura, Y. *et al.* (2002) Functional SNPs in the lymphotoxin-α gene that are associated with susceptibility to myocardial infarction. *Nat. Genet.*, **32**, 650–654.
20. Iida, A., Saito, S., Sekine, A., Mishima, C., Kondo, K., Kitamura, Y., Harigae, S., Osawa, S. and Nakamura, Y. (2001) Catalog of 258 single-nucleotide polymorphisms (SNPs) in genes encoding three organic anion transporters, three organic anion-transporting polypeptides, and three NADH: ubiquinone oxidoreductase flavoproteins. *J. Hum. Genet.*, **46**, 668–683.
21. Yamada, R., Tanaka, T., Unoki, M., Nagai, T., Sawada, T., Ohnishi, Y., Tsunoda, T., Yukioka, M., Maeda, A., Suzuki, K. *et al.* (2001) Association between a single-nucleotide polymorphism in the promoter of the human interleukin-3 gene and rheumatoid arthritis in Japanese patients, and

maximum-likelihood estimation of combinatorial effect that two genetic loci have on susceptibility to the disease. *Am. J. Hum. Genet.*, **68**, 674–685.
22. Devlin, B. and Risch, N. (1995) A comparison of linkage disequilibrium measures for fine-scale mapping. *Genomics*, **29**, 311–322.
23. Excoffier, L. and Slatkin, M. (1995) Maximum-likelihood estimation of molecular haplotype frequencies in a diploid population. *Mol. Biol. Evol.*, **12**, 921–927.
24. Nakajima, M., Kizawa, H., Saitoh, M., Kou, I., Miyazono, K. and Ikegawa, S. (2007) Mechanisms for asporin function and regulation in articular cartilage. *J. Biol. Chem.*, **282**, 32185–32192.
25. Andrews, N.C. and Faller, D.V. (1991) A rapid micropreparation technique for extraction of DNA-binding proteins from limiting numbers of mammalian cells. *Nucleic Acids Res.*, **19**, 2499.
26. Lee, W., Mitchell, P. and Tjian, R. (1987) Purified transcription factor AP-1 interacts with TPA-inducible enhancer elements. *Cell*, **49**, 741–752.
27. Tokuhiro, S., Yamada, R., Chang, X., Suzuki, A., Kochi, Y., Sawada, T., Suzuki, M., Nagasaki, M., Ohtsuki, M., Ono, M. *et al.* (2003) An intronic SNP in a *RUNX1* binding site of *SLC22A4*, encoding an organic cation transporter, is associated with rheumatoid arthritis. *Nat. Genet.*, **35**, 341–348.

Table 1. Healthy Donors and Patients[a]

	M/F	Age (years)	WBC	CRP	RF	Resting MFI	Activated MFI
Healthy donor (n = 28)	17/11	21.5 ± 1.1 (19-23)	5050 ± 1043 (3500-7700)	No data	No data	28.57 ± 18.83 (9.59-87.98)	113.77 ± 64.47 (25.35-273.21)
RA patient (n = 20)							
Without infliximab (n = 8)	0/8	51.9 ± 5.9 (44-64)	8100 ± 2538 (4000-11 100)	0.6 ± 0.8 (0.0-2.4)	21.0 ± 20.1 (5-58)	101.80 ± 43.67 (31.35-165.89)	181.96 ± 50.17 (117.93-273.93)
With infliximab (n = 12)	1/11	54.1 ± 7.7 (43-67)	8025 ± 2650 (4100-11 500)	2.3 ± 3.1 (0.0-11.1)	43.8 ± 71.7 (0-239)	39.82 ± 24.09 (12.30-96.95)	153.89 ± 76.65 (34.81-286.01)
Infection (n = 29)	25/4	58.4 ± 18.1 (20-84)	15 227 ± 5415 (10 060-28 630)	16.7 ± 5.3 (10.0-27.9)	No data	165.09 ± 102.78 (23.70-570.60)	370.11 ± 185.33 (40.21-738.58)

NOTE: WBC = white blood cell; CRP = C-reactive protein; RF = rheumatoid factor; MFI = mean fluorescence intensity; RA = rheumatoid arthritis.
[a]Data in parentheses refer to threshold ranges.

Table 2. Patients With Rheumatoid Arthritis

No.	Age (years)	Sex	Infliximab Infusion Count	WBC (per ?L)	CRP (mg/dL)	RF (IU/mL)	%PR3-high[a]	Resting MFI	Activated MFI
1	51	F	None	8900	0.2	5	70.62	31.35	143.24
2	44	F	None	8400	0.5	9	60.25	48.87	117.93
3	53	F	None	11 100	1.1	34	94.21	101.39	173.56
4	51	F	None	10 200	0.1	5	64.46	107.39	168.53
5	55	F	None	10 300	0.1	8	61.49	107.93	170.69
6	49	F	None	6100	2.4	7	74.52	114.45	273.93
7	64	F	None	5800	0.0	42	74.52	137.13	170.54
8	48	F	None	4000	0.5	58	69.74	165.89	237.23
9	57	F	2	4100	0.0	1	69.07	28.35	168.43
10	56	F	3	9400	4.1	239	18.33	12.30	41.97
11	67	F	3	5100	3.9	56	71.86	56.57	238.16
12	56	F	3	4800	0.8	0	78.74	96.95	157.55
13	67	F	4	9300	0.5	25	54.65	65.75	124.79
14	49	F	5	6300	1.5	4	88.92	30.38	241.52
15	43	F	5	9600	2.0	133	70.95	41.44	286.01
16	55	F	5	11 500	1.7	15	69.08	46.17	181.11
17	53	F	6	6500	0.0	22	97.11	16.43	34.81
18	55	F	6	11 500	11.1	13	36.81	18.53	98.67
19	45	F	6	10 700	1.7	13	58.25	28.18	148.00
20	46	M	6	7500	0.9	5	95.61	36.80	125.68

NOTE: WBC = white blood cell; CRP = C-reactive protein; RF = rheumatoid factor; MFI = mean fluorescence intensity.
[a]%PR3-high: the percentage of PR3 high-expression neutrophils.

In Vitro Stimulation Experiments and the Measurement of Membrane PR3 Expression by Flow Cytometry

The isolated neutrophils were resuspended in HBSS+ buffer at a final concentration of 2×10^6/mL. The cell suspension was incubated with various stimuli in polypropylene tubes and then washed with 1 mL ice-cold HBSS+ buffer. Both during and after incubation, various inhibitors such as plasma were added and then washed with 1 mL ice-cold HBSS+ buffer. The cells were pelleted and resuspended in HBSS+ buffer before they were incubated with a dilution of monoclonal Alexa 488–labeled antibody to PR3 in polystyrene tubes. Data acquisition by flow cytometry and subsequent analyses were done on the same day with a FACScan using the CellQuest software package (Becton Dickinson, Heidelberg, Germany). Neutrophils were gated according to their relative size (forward scatter) and relative granularity (side scatter) properties.

All data were reported as the mean fluorescence intensity (MFI), thus reflecting the total amount of membrane PR3 expression.

Statistical Analysis

Differences in the continuous variables between the two groups were analyzed by means of the Mann–Whitney *U* test. Two-sided $P < .05$ was considered to be statistically significant.

Results

Figure 1 shows the membrane PR3 expression on neutrophils from a healthy donor and 3 patients with inflammatory disease. Purified neutrophils were stained for membrane PR3 either with stimulation (activated) or without stimulation (resting) by 1 ng/mL TNF-α and 1 μM FMLP in vitro. Membrane PR3 expression on neutrophils increased after stimulation in vitro; however, the expression without stimulation was very small. Membrane PR3 expression from patients with infection (Figure 1B) or RA patients without infliximab therapy (Figure 1C) was much larger than in healthy donors (Figure 1A) regardless of whether or not stimulation was performed in vitro. Membrane PR3 expression on neutrophils from RA patients with infliximab therapy was less than in those without it (Figure 1C) in a resting state, but it increased after stimulation in vitro (Figure 1D).

Increasing Membrane PR3 Expression on Neutrophil Stimulated by Various Proinflammatory Cytokines In Vitro

Figure 2 shows the amount of membrane PR3 expression on neutrophils from healthy donors with various stimuli for 20 minutes at 37°C. Membrane PR3 expression (MFI) significantly increased after incubation with various proinflammatory cytokines such as TNF-α (10 ng/mL), IL-1β (10 ng/mL), IL-6 (10 ng/mL), IL-8 (10 ng/mL), and IFN-α (20 U/mL).

The Suppression of Membrane PR3 Expression on Neutrophils by Plasma and Protease Inhibitor

Purified neutrophils from 3 healthy donors were stimulated by 1 ng/mL TNF-α and 1 μM FMLP with or without plasma from healthy donors or 10 μM α_1PI. The increase in membrane PR3 expression after stimulation by TNF and FMLP was significantly suppressed by plasma or α_1PI but not APC or AT (Figure 3).

Neutrophil Membrane PR3 Expression From Healthy Donors, Patients With RA, or Patients With Infectious Disease

Figure 4 shows membrane PR3 expression on neutrophils from patients with RA or infectious diseases. Membrane PR3 expression on neutrophils in patients with infection (165.09 ± 102.78) and RA patients without infliximab therapy (101.80 ± 43.67) were significantly higher than in healthy donors (28.57 ± 18.83). Remarkably, membrane PR3 expression in RA patients with infliximab therapy (39.82 ± 24.09) was significantly lower than in those without it. In addition, the condition of the patients with RA improved after treatment with infliximab.

Discussion

Previous reports have shown that an elevated level of membrane PR3 expression is related to disease and relapse in patients with PR3-ANCA-associated vasculitis containing WG.[12-14] Our findings have shown that membrane PR3 expression on neutrophils is significantly higher in patients with more common diseases, such as infection or RA. These patients did not include those with PR3-ANCA-associated vasculitis. PR3 expression on neutrophils increased in relation to the C-reactive protein (CRP) concentration (data not shown). A previous study reported that PR3 expression on neutrophils closely correlated with CRP in patients with infections.[9] These findings suggest that an elevated expression of PR3 on neutrophils is a good marker, which may also play an important role in these diseases. Elevated levels of cytokines, such as TNF-α, have been reported in RA patients[15] and in septic patients with disseminated intravascular coagulation.[16]

The amount of PR3 expression on neutrophils significantly increased with the addition of various cytokines such as TNF-α, IL-1β, IL-6, IL-8, or IFN-α. A previous report showed that membrane PR3 expression on neutrophils was upregulated by proinflammatory mediators such as TNF-α, IL-1β, or IL-6.[17] TNF-α is produced as a membrane-bound proform,

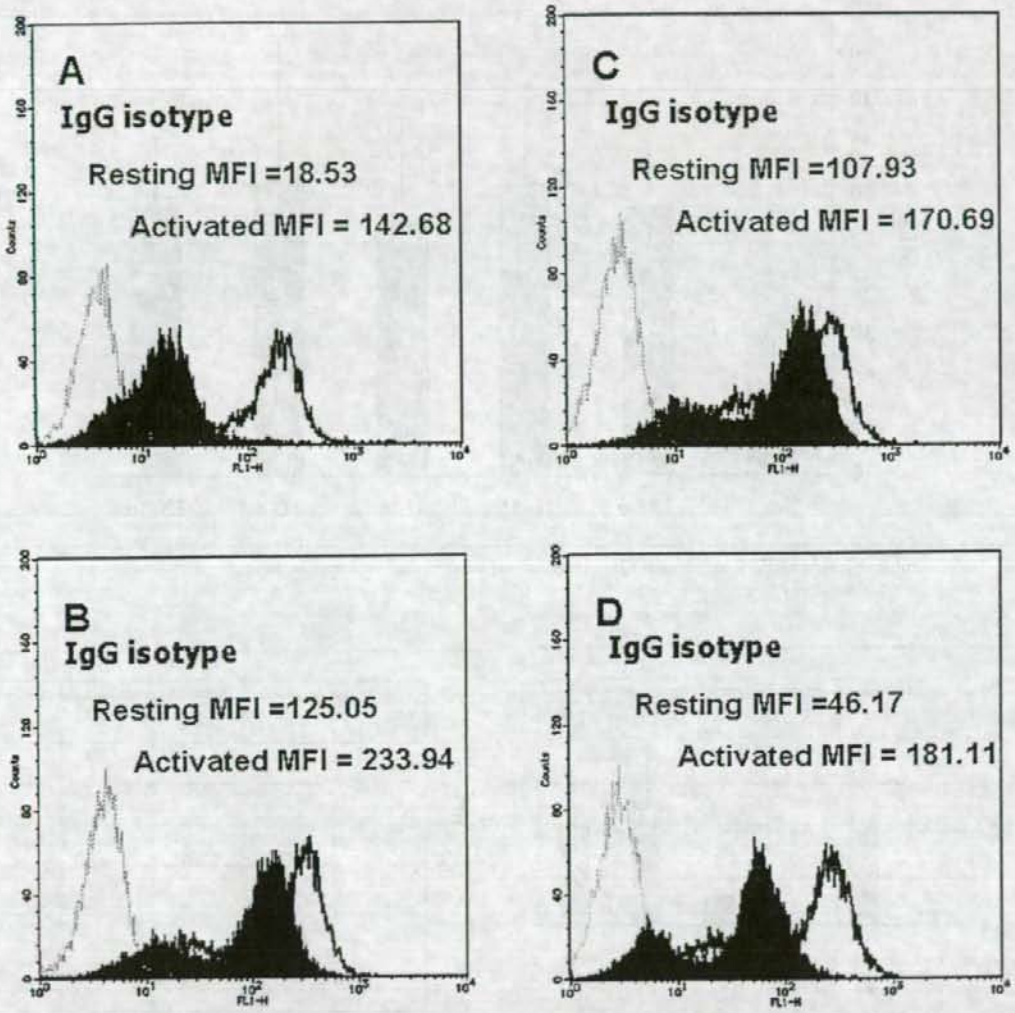

Figure 1. Neutrophil membrane PR3 expression observed in a healthy donor and in patients with inflammatory disease. The isotype control showed no significant membrane staining. Purified neutrophils were stained for membrane PR3 with stimulation (activated MFI) or without stimulation (filled; resting MFI) in vitro.

which needs to be cleaved proteolytically to be released in its major biologically active form. PR3 is able to process TNF-α in vitro into its active form.[18] The expression of PR3 on neutrophils was markedly suppressed with the addition of plasma. The expression of PR3 was suppressed by α_1PI but not AT or APC. These findings are consistent with those of previous reports,[19] indicating that the main inhibitor of membrane PR3 on neutrophils is α_1PI. α_1PI, which is mainly synthesized in the liver and occurs in high concentrations in plasma, inhibits PR3 activity very quickly.[20]

Anti-TNF-α treatment has been reported to be successful in patients with RA.[9,10] Our present findings show that membrane PR3 expression on neutrophils is downregulated in RA patients by treatment with infliximab, suggesting that anti-TNF antibody suppresses PR3 expression in RA patients. Therefore, after activation with TNF-a and FMLP, no significant difference was observed between RA

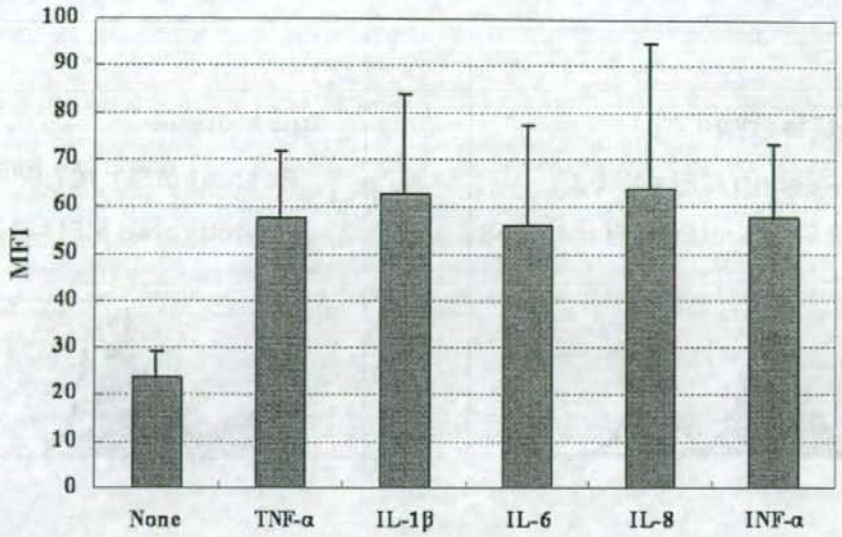

Figure 2. Neutrophil membrane PR3 expression after stimulation by various cytokines in vitro.

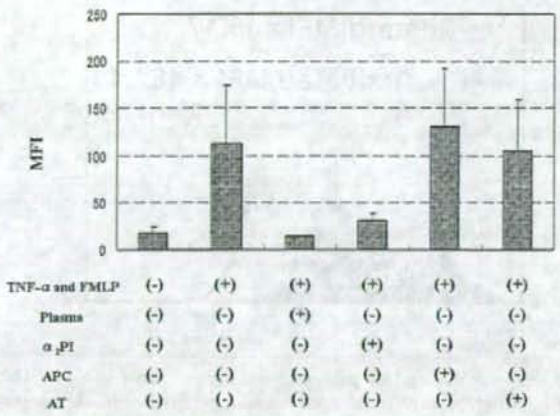

Figure 3. Neutrophil membrane PR3 expression after stimulation by 1 ng/mL TNF-α and 1 μM FMLP.

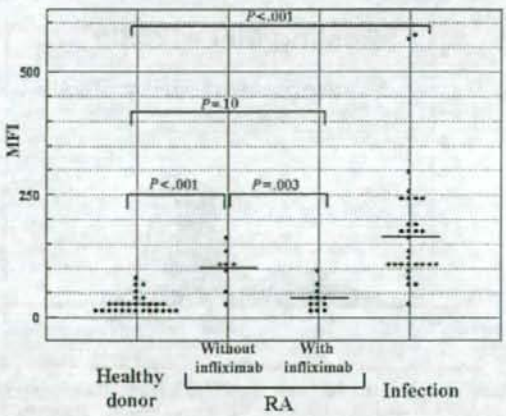

Figure 4. Neutrophil membrane PR3 expression from healthy donors, patients with RA, or patients with infectious disease.

patients with and without treatment with Remicade. These findings show that the addition of TNF neutralizes anti-TNF antibodies in patients. In these patients, both the condition of the patients and CRP concentration improved. Thus, anticytokine therapy or substitution therapy using protease inhibitors might be more effective for the treatment of infectious diseases in which PR3 is related to the clinical condition. Indeed, infliximab was reported to be effective in the treatment of a case of refractory WG by improving the kidney function and also inducing clinical remission.[21]

Membrane PR3 expression on neutrophils in an RA patient was downregulated by anti-TNF antibody therapy. Therefore, PR3 might play an important role in the neutrophil-mediated inflammatory reaction

not only in PR3-ANCA-associated vasculitis but also in more common diseases such as RA and infection.

Acknowledgments

This work was supported in part by a grant-in-aid for Blood Coagulation Abnormalities from the Ministry of Health, Labour and Welfare of Japan.

References

1. Jenne DE, Tschopp J, Ludemann J, Utecht B, Gross WL. Wegener's autoantigen decoded. *Nature*. 1990; 346:520.
2. Labbaye C, Musette P, Cayre YE. Wegener autoantigen and myeloblastin are encoded by a single mRNA. *Proc Natl Acad Sci U S A*. 1991;88:9253-9256.
3. Csernok E, Ernst M, Schmitt W, Bainton DF, Gross WL. Activated neutrophils express proteinase 3 on their plasma membrane in vitro and in vivo. *Clin Exp Immunol*. 1994;95:244-250.
4. Witko-Sarsat V, Cramer EM, Hieblot C, et al. Presence of proteinase 3 in secretory vesicles: evidence of a novel, highly mobilizable intracellular pool distinct from azurophil granules. *Blood*. 1999;94:2487-2496.
5. Bajema IM, Hagen EC, van der Woude FJ, Bruijn JA. Wegener's granulomatosis: a meta-analysis of 349 literary case reports. *J Lab Clin Med*. 1997;129:17-22.
6. Hoffman GS, Drucker Y, Cotch MF, Locker GA, Easley K, Kwoh K. Wegener's granulomatosis: patient-reported effects of disease on health, function, and income. *Arthritis Rheum*. 1998;41:2257-2262.
7. van Rossum AP, Rarok AA, Huitema MG, Fassina G, Limburg PC, Kallenberg CG. Constitutive membrane expression of proteinase 3 (PR3) and neutrophil activation by anti-PR3 antibodies. *J Leukoc Biol*. 2004;76: 1162-1170.
8. Jennette JC. Renal involvement in systemic vasculitis. In Jennette JC, Olson JL, Schwartz MM, Silva FG, eds. *Heptinstall's Pathology of the Kidney*. Philadelphia, PA: Lippincott-Raven; 1998:1059-1095.
9. Matsumoto T, Kaneko T, Wada H, et al. Proteinase 3 expression on neutrophil membranes from patients with infectious disease. *Shock*. 2006;26:128-133.
10. Feldmann M. Development of anti-TNF therapy for rheumatoid arthritis. *Nat Rev Immunol*. 2002;2:364-371.
11. Lipsky PE, van der Heijde DM, St Clair EW, et al. Infliximab and methotrexate in the treatment of rheumatoid arthritis. Anti-Tumor Necrosis Factor Trial in Rheumatoid Arthritis with Concomitant Therapy Study Group. *N Engl J Med*. 2000;343:1594-1602.
12. Uehara A, Sugawara Y, Sasano T, Takada H, Sugawara S. Proinflammatory cytokines induce proteinase 3 as membrane-bound and secretory forms in human oral epithelial cells and antibodies to proteinase 3 activate the cells through protease-activated receptor-2. *J Immunol*. 2004; 173:4179-4189.
13. Duranton J, Bieth JG. Inhibition of proteinase 3 by α1-antitrypsin in vitro predicts very fast inhibition in vivo. *Am J Respir Cell Mol Biol*. 2003;29:57-61.
14. Feldmann M, Maini RN. The role of cytokines in the pathogenesis of rheumatoid arthritis. *Rheumatology (Oxford)*. 1999;38(suppl 2):3-7.
15. Robache-Gallea S, Morand V, Bruneau JM, et al. In vitro processing of human tumor necrosis factor-alpha. *J Biol Chem*. 1995;270:23688-23692.
16. Wada H, Ohiwa M, Kaneko T, et al. Plasma level of tumor necrosis factor in disseminated intravascular coagulation. *Am J Hematol*. 1991;37:147-151.
17. Muller Kobold AC, Kallenberg CG, Tervaert JW. Leucocyte membrane expression of proteinase 3 correlates with disease activity in patients with Wegener's granulomatosis. *Br J Rheumatol*. 1998;37:901-907.
18. Rarok AA, Stegeman CA, Limburg PC, Kallenberg CG. Neutrophil membrane expression of proteinase 3 (PR3) is related to relapse in PR3-ANCA-associated vasculitis. *J Am Soc Nephrol*. 2002;13:2232-2238.
19. van Rossum AP, Limburg PC, Kallenberg CG. Membrane proteinase 3 expression on resting neutrophils as a pathogenic factor in PR3-ANCA-associated vasculitis. *Clin Exp Rheumatol*. 2003;21(6, suppl 32):S64-S68.
20. Campbell EJ, Campbell MA, Owen CA. Bioactive proteinase 3 on the cell surface of human neutrophils: quantification, catalytic activity, and susceptibility to inhibition. *J. Immunol*. 2000;165:3366-3374.
21. Kleinert J, Lorenz M, Kostler W, Horl W, Sunder-Plassmann G, Soleiman A. Refractory Wegener's granulomatosis responds to tumor necrosis factor blockade. *Wien Klin Wochenschr*. 2004;116:334-338.

ORTHO SUPERSITE

Bilateral Subchondral Insufficiency Fracture of the Femoral Head

By Akihiro Sudo, MD; Masahiro Hasegawa, MD; Ko Kato, MD; Atsumasa Uchida, MD
ORTHOPEDICS 2008; 31:399

April 2008

Subchondral insufficiency fracture of the femoral head is an infrequent cause of acute hip pain in elderly women with osteoporosis. This condition is easily confused with osteonecrosis, transient osteoporosis of the hip, or rapidly destructive coxarthrosis. These diseases are bilateral, yet almost all previous reports of this condition have documented unilateral cases.[1-9] This article reports the clinical and histological features of bilateral subchondral insufficiency fracture of the femoral head in a 68-year-old woman.

Case Report

A 68-year-old woman suddenly experienced pain in her left hip without apparent trauma on October 23, 2001. Because walking exacerbated the pain, she presented to our department on 3 days later. She reported having undergone a mitral commissurotomy for the treatment of mitral valve stenosis in 1972, approximately 29 years prior to presentation. Ten years later, she had a cerebral infarction with left hemiparesis. She had no history of steroid use or alcoholism. Radiographs of the patient's left hip showed that the center-edge angle was 20°, suggesting mild acetabular dysplasia. No other abnormality was seen. The patient was treated with anti-inflammatory drugs. However, when she visited our department again on November 9, 2001, radiographs showed a subchondral collapse of the left femoral head (Figure 1A). Consequently, the patient was admitted on November 26, 2001.

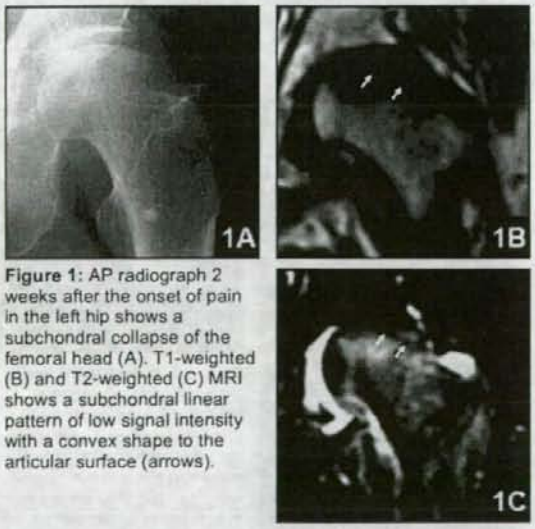

Figure 1: AP radiograph 2 weeks after the onset of pain in the left hip shows a subchondral collapse of the femoral head (A). T1-weighted (B) and T2-weighted (C) MRI shows a subchondral linear pattern of low signal intensity with a convex shape to the articular surface (arrows).

The patient was 154 cm tall, weighed 63 kg, and was slightly obese with a body mass index of 27.3. While the range of motion of the left hip was not markedly restricted, her walking ability and daily living activity were severely restricted. The bone mineral density of the lumbar spine, as assessed by dual energy radiographic absorptiometry, was 74% of the mean in young adults, and a compression fracture of Th12 was seen on a radiograph of the thoracic spine, indicating osteoporosis. The bone mineral densities of the left and right femoral necks were 75% and 72%, respectively, of the mean in young adults.

On magnetic resonance imaging (MRI), the entire femoral head was depicted as a low intensity area on a T1-weighted image, and there was a subchondral linear pattern of low signal intensity with a convex shape to the articular surface (Figure 1B). On a T2-weighted image, the entire femoral head was depicted as a high intensity area; as on the T1-weighted image, a linear low signal intensity pattern was noted (Figure 1C). Computed

tomography showed a low-density area, which was suspected to be a fracture line in the left femoral head. On the basis of these findings, subchondral insufficiency fracture of the left femoral head was diagnosed. After medical treatment including the discontinuation of warfarin therapy, the patient underwent hemiarthroplasty on December 17, 2001. Hemiarthroplasty was selected because the acetabular cartilage had a normal appearance.

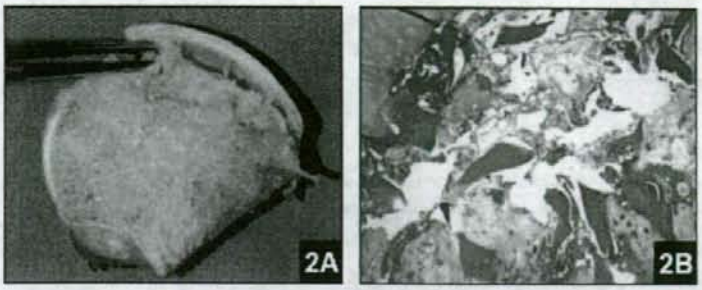

Figure 2: A cross-section of the femoral head shows that the articular cartilage with attached subchondral bone is detached in the superior portion of the femoral head. Fracture line is identified in the subchondral area (A). Photomicrograph shows a partial trabecular rupture and destruction surrounded by fracture callus and granulation tissue (×40; B).

The surface cartilage of the excised femoral head was wrinkled. The cross-section showed that the articular cartilage with attached subchondral bone was detached in the superior portion of the femoral head, and a fracture line was identified in the subchondral area (Figure 2A). Histologically, a partial trabecular rupture and destruction surrounded by fracture callus and granulation tissue were seen, but findings indicative of bone necrosis were not observed (Figure 2B). In addition, the trabecula was generally narrow and exhibited findings indicative of osteoporosis.

Although the patient's postoperative course was favorable, she experienced idiopathic pain in the right hip region while undergoing rehabilitation at another hospital. No abnormal findings were seen in the right knee or hip on radiographs taken on February 1, 2002, but a lateral radiograph of the hip taken on March 19 showed an irregularity at the surface of the right femoral head, suggesting a subchondral fracture (Figure 3A). The patient was advised to use crutches. However, she was readmitted to our hospital on April 18 because of an intractable severity of the pain.

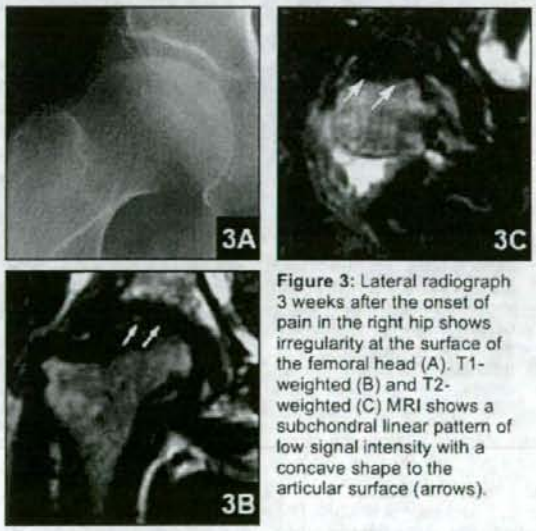

Figure 3: Lateral radiograph 3 weeks after the onset of pain in the right hip shows irregularity at the surface of the femoral head (A). T1-weighted (B) and T2-weighted (C) MRI shows a subchondral linear pattern of low signal intensity with a concave shape to the articular surface (arrows).

A tomogram of the right hip taken after admission clearly showed a compressed femoral head and peripheral irregularity. On MRI of the hip, the entire head was depicted as a low intensity area on T1-weighted imaging, and there was a subchondral linear pattern of low signal intensity with a concave shape to the articular surface (Figure 3B). On T2-weighted imaging, the entire femoral head was depicted as a high intensity area, with the exception of a low intensity area at the apex (Figure 3C). On May 2, hemiarthroplasty was performed. We selected hemiarthroplasty again because the acetabular cartilage appeared normal.

The lateral portion of the articular cartilage of the excised femoral head was only slightly wrinkled. Cross-sections of the femoral head showed a concave fracture line in the subchondral bone underneath the weight-bearing area surrounded by a reddish area (Figure 4A). Histologically, trabecular rupture and destruction surrounded by fracture callus and granulation tissue were seen underneath the cartilage, but no findings of bone necrosis were seen (Figure 4B). Pain in the right hip disappeared after surgery.

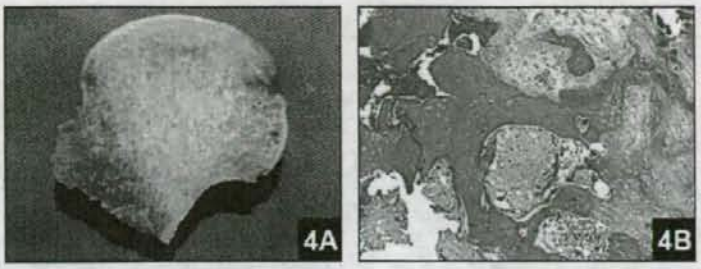

Figure 4: A cross-section of the femoral head shows that the fracture line is identified in the subchondral area (A). Photomicrograph shows an abundant fracture callus (×100; B).

Discussion

Subchondral fractures of the femoral head have been rarely reported as a "stress fracture of the femoral head."[10] In 1996, Bangil et al [1] first named this lesion "subchondral insufficiency fracture of the femoral head." The clinical characteristics of subchondral insufficiency fractures of the femoral head may be considered as follows. The patients usually are elderly, obese women with osteoporosis who have an acute onset of hip pain without history of trauma, steroid use, and alcoholism. In the early stage, plain radiographic results can be normal. However, MRI reveals the focal low-intensity band on T1-weighted and T2-weighted images that reflects the fracture line with a pattern of bone marrow edema.

Almost all of the documented cases of subchondral insufficiency fracture of the femoral head have been unilateral. Rafii et al[11] reported 3 cases of insufficiency fracture of the femoral head, and, while 1 case was bilateral, the fracture was subcapital, not subchondral. Ikemura et al[12] reported a bilateral case after renal transplantation. In the present patient, the insufficiency fracture was subchondral in bilateral femoral heads without a history of renal disorder. This 68-year-old woman was obese with a body mass index of 27.3 and had a compression fracture of the spine, indicating osteoporosis. The center-edge angle was 20° on both hips. Although the patient had mild left hemiparesis, bone mineral densities of both femoral necks were almost the same. Namely, the conditions of both femoral heads were the same. From this background information, it is not strange that this lesion is seen on bilateral hips.

The differential diagnosis includes osteonecrosis and transient osteoporosis of the hip. On MRI, it is difficult to distinguish between osteonecrosis and a subchondral insufficiency fracture. It is reported that the shape of the low intensity band is different. That is, the shape in osteonecrosis is concave to the articular surface, whereas in a subchondral insufficiency fracture, the shape is usually convex to the articular surface. However, several authors have reported subchondral insufficiency fractures in which the shape of the low intensity band is concave to the articular surface.[1,2,7] In our patient, the left side was convex and the right side was concave. Osteonecrosis was ruled out histologically.

In transient osteoporosis of the hip, MRI shows bone marrow edema and linear patterns of low signal intensity in the subchondral area on T1-weighted images, thought to represent fracture lines. Miyanishi et al[13] reported that the presence of a subchondral fracture might be important when considering the pathophysiology of transient osteoporosis of the hip. This condition is self-limiting, and bilateral cases are reported occasionally. Transient osteoporosis commonly affects healthy middle-aged men as well as women during the third trimester of pregnancy, but a subchondral insufficiency fracture does not. The relationship between these conditions is controversial and needs further investigation.

Rapidly destructive coxarthrosis is a rare disease that most frequently affects women with osteoporosis. Recently, several studies have reported that some cases of subchondral insufficiency fracture occasionally result in rapidly destructive coxarthrosis.[4,9] We also observed another case of insufficiency fracture, diagnosed from the results of MRI, that progressed to rapid hip destruction despite no weight-bearing being allowed on the affected lower extremity. That patient's background of subchondral insufficiency fracture and rapidly destructive coxarthrosis was quite similar to the patient's background in this case. We also believe that subchondral insufficiency fracture seems to an important factor involved in the pathogenesis of rapidly destructive coxarthrosis.

While the reason for the lack of bilateral cases of subchondral insufficiency fracture is not known, there have been

reports of bilateral rapidly destructive coxarthrosis. As more cases of subchondral insufficiency fracture are documented, we may find more bilateral cases appearing in the literature.

References

1. Bangil M, Soubrier M, Dubost JJ, et al. Subchondral insufficiency fracture of the femoral head. *Rev Rhum Engl Ed*. 1996; 63(11):859-861.
2. Hagino H, Okano T, Teshima R, Nishi T, Yamamoto K. Insufficiency fracture of the femoral head in patients with severe osteoporosis: report of 2 cases. *Acta Orthop Scand*. 1999; 70(1):87-89.
3. Motomura G, Yamamoto T, Miyanishi K, Shirasawa K, Noguchi Y, Iwamoto Y. Subchondral insufficiency fracture of the femoral head and acetabulum : a case report. *J Bone Joint Surg Am*. 2002; 84(7):1205-1209.
4. Watanabe W, Itoi E, Yamada S. Early MRI findings of rapidly destructive coxarthrosis. *Skeletal Radiol*. 2002; 31(1):35-38.
5. Yamamoto T, Bullough PG. Subchondral insufficiency fracture of the femoral head and medial femoral condyle. *Skeletal Radiol*. 2000; 29(1):40-44.
6. Yamamoto T, Bullough PG. Spontaneous osteonecrosis of the knee: the result of subchondral insufficiency fracture. *J Bone Joint Surg Am*. 2000; 82(6):858-866.
7. Yamamoto T, Schneider R, Bullough PG. Insufficiency subchondral fracture of the femoral head. *Am J Surg Pathol*. 2000; 24(3):464-468.
8. Yamamoto T, Schneider R, Bullough PG. Subchondral insufficiency fracture of the femoral head: histopathologic correlation with MRI. *Skeletal Radiol*. 2001; 30(5):247-254.
9. Yamamoto T, Takabatake K, Iwamoto Y. Subchondral insufficiency fracture of the femoral head resulting in rapid destruction of the hip joint: a sequential radiographic study. *AJR Am J Roentgenol*. 2002; 178(2):435-437.
10. van Linthoudt D, Ott H. Supraacetabular and femoral head stress fracture during fluoride treatment. *Gerontology*. 1987; 33(5):302-306.
11. Rafii M, Mitnick H, Klug J, Firooznia H. Insufficiency fracture of the femoral head: MR imaging in three patients. *AJR Am J Roentgenol*. 1997; 168(1):159-163.
12. Ikemura S, Yamamoto T, Nakashima Y, Shuto T, Jingushi S, Iwamoto Y. Bilateral subchondral insufficiency fracture of the femoral head after renal transplantation: a case report. *Arthritis Rheum*. 2005; 52(4):1293-1296.
13. Miyanishi K, Yamamoto T, Nakashima Y, et al. Subchondral changes in transient osteoporosis of the hip. *Skeletal Radiol*. 2001; 30(5):255-261.

Authors

Drs Sudo, Hasegawa, Kato, and Uchida are from Department of Orthopedic Surgery, Mie University, Graduate School of Medicine, Mie, Japan.

Drs Sudo, Hasegawa, Kato, and Uchida have no relevant financial relationships to disclose.

Correspondence should be addressed to: Akihiro Sudo, MD, Department of Orthopedic Surgery, Mie University, Graduate School of Medicine, 2-174 Edobashi, Tsu City, Mie 514-8507, Japan.

nature genetics

Common variants in *DVWA* on chromosome 3p24.3 are associated with susceptibility to knee osteoarthritis

Yoshinari Miyamoto[1], Dongquan Shi[2], Masahiro Nakajima[1], Kouichi Ozaki[3], Akihiro Sudo[4], Akihiro Kotani[5], Atsumasa Uchida[4], Toshihiro Tanaka[3], Naoshi Fukui[6], Tatsuhiko Tsunoda[7], Atsushi Takahashi[8], Yusuke Nakamura[9], Qing Jiang[2] & Shiro Ikegawa[1]

Susceptibility to osteoarthritis, the most common human arthritis, is known to be influenced by genetic factors[1,2]. Through a genome-wide association study using ~100,000 SNPs, we have identified a previously unknown gene on chromosome 3p24.3, *DVWA*, which is associated with susceptibility to knee osteoarthritis. Expressed specifically in cartilage, *DVWA* encodes a 276-amino-acid protein with two regions corresponding to the von Willebrand factor type A domain (VWA domain)[3]. Several *DVWA* SNPs are significantly associated with knee osteoarthritis in two independent Japanese case-control cohorts. This association was replicated in a Japanese population cohort and a Han Chinese case-control cohort (combined $P = 7.3 \times 10^{-11}$). DVWA protein binds to β-tubulin, and the binding is influenced by two highly associated missense SNPs (rs11718863 and rs7639618) located in the VWA domain. The Tyr169-Cys260 isoform of DVWA, which is overrepresented in knee osteoarthritis, showed weaker interaction. Our findings reveal a new paradigm for study of osteoarthritis etiology and pathogenesis.

Osteoarthritis (MIM165720) is a common disorder that causes pain and restricted motion in joints, particularly the knee and hip[4]. About 6% of adults age 30 and older have frequent knee pain and radiographic osteoarthritis[5]. In the elderly, osteoarthritis frequently leads not only to disability but also to financial difficulty[6,7]. The critical need to manage osteoarthritis worldwide is the focus of the current 'Bone and Joint Decade' campaign. Susceptibility to osteoarthritis is influenced by genetic predisposition[8] and multiple susceptibility genes[1,2]. A few associated genes, including *FRZB*[9], *ASPN*[10] and *GDF5* (ref. 11), were identified using the candidate gene approach and confirmed in multiple populations, with functional data supporting their causality[1,12,13]. However, the genetic contribution to this complex disease is not entirely known.

The genome-wide association study is a powerful means for dissecting complex human diseases such as osteoarthritis. Susceptibility genes for several common diseases have been identified using this approach[14–16]. Notable advantages include its comprehensiveness and the potential for finding susceptibility genes with previously unknown function and relationship to the disease. As a part of the Japanese Millennium Project[14,17], we carried out a genome-wide association study for knee osteoarthritis.

To begin the study, we genotyped 94 knee osteoarthritis cases and 658 controls (set A) using 99,295 SNPs selected from the JSNP database[17]. After confirming the data quality, we compared the results of 79,763 SNPs between cases and controls by χ^2 tests for genotype, dominant, recessive and allele frequency models. We identified 2,153 SNPs that showed P values less than 0.01 in any of the four models. We further genotyped these SNPs using an independent population consisting of 646 knee osteoarthritis cases and 631 controls (set B). The SNP rs3773472 showed strong association (**Table 1**). This finding remained significant after Bonferroni correction ($0.000017 \times 2{,}153 = 0.037$). Therefore, we decided to examine SNPs around rs3773472. There were no other SNPs that showed significant association.

We referenced the International HapMap Project database (release 21a) and selected SNPs with D' value of >0.7 to rs3773472 and with a minor allele frequency of >0.1. The linkage disequilibrium (LD) block around rs3773472 contained 40 HapMap SNPs, two validated genes (*SH3BP5* and *CAPN7*) and one predicted gene (*LOC344875*). Next, we selected 12 tag SNPs (including rs3773472) that covered all 40 SNPs with an r^2 value of >0.9. After genotyping the tag SNPs using population set B, we found a more significantly associated SNP, rs7639618 ($P = 7.3 \times 10^{-8}$; **Table 2**). We examined potential

[1]Laboratory for Bone and Joint Diseases, Center for Genomic Medicine, RIKEN, 4-6-1 Shirokanedai, Minato-ku, Tokyo 108-8639, Japan. [2]The Center of Diagnosis and Treatment for Joint Disease, Drum Tower Hospital Affiliated to Medical School of Nanjing University, Zhongshan Road 321, Nanjing 210008, Jiangsu, China. [3]Laboratory for Cardiovascular Diseases, Center for Genomic Medicine, RIKEN, 1-7-22 Suehiro-cho, Tsurumi-ku, Yokohama, Kanagawa 230-0045, Japan. [4]Department of Orthopaedic Surgery, Mie University Faculty of Medicine, 2-174 Edobashi, Tsu, Mie 514-8507, Japan. [5]Department of Orthopaedic Surgery, Kyorin University, School of Medicine, 6-20-2 Shinkawa, Mitaka, Tokyo 181-8611, Japan. [6]Department of Pathomechanisms, Clinical Research Center for Rheumatology and Allergy, National Hospital Organization Sagamihara National Hospital, 18-1 Sakuradai, Sagamihara 228-8522, Japan. [7]The Laboratory for Medical Informatics, Center for Genomic Medicine, RIKEN, 1-7-22 Suehiro-cho, Tsurumi-ku, Yokohama, Kanagawa 230-0045, Japan. [8]Laboratory for Statistical Analysis, Center for Genomic Medicine, RIKEN, 4-6-1 Shirokanedai, Minato-ku, Tokyo 108-8639, Japan. [9]Laboratory for Genotyping, Center for Genomic Medicine, RIKEN, 4-6-1 Shirokanedai, Minato-ku, Tokyo 108-8639, Japan. Correspondence should be addressed to S.I. (sikegawa@ims.u-tokyo.ac.jp).

Received 27 August 2007; accepted 5 May 2008; published online 11 July 2008; doi:10.1038/ng.176

Table 1 Association of rs3773472 with knee osteoarthritis in the genome-wide analysis

	Case					Control					
	Genotype					Genotype					
Population	CC	CG	GG	Sum	Allele G frequency	CC	CG	GG	Sum	Allele G frequency	*P* value for allele frequency
Set A	52	37	5	94	0.250	259	279	77	615	0.352	0.0059
Set B	324	272	50	646	0.288	240	314	74	628	0.368	0.000017
Set A+B combined	376	309	55	740	0.283	499	593	151	1243	0.360	0.00000065

confounding factors such as age, body mass index (BMI) and sex to evaluate whether they could generate pseudo-positive associations. No significant differences in mean age, BMI and sex distribution were apparent among rs7639618 genotypes (**Supplementary Table 1** online). We also checked for a population stratification effect using a genomic control method[18,19] but found this an unlikely explanation for the positive association (**Supplementary Table 2** online).

To confirm the association, we examined an independent population cohort (set C), which was divided into knee osteoarthritis and control groups on the basis of knee radiographs. Genotyping of rs7639618 in 242 knee osteoarthritis cases and 485 controls produced another significant result (**Table 3**). We further examined the association of rs7639618 in a Han Chinese population consisting of 417 knee osteoarthritis cases and 413 controls. The association was replicated in this distinct population ($P = 0.00072$; **Table 3**), further establishing the association of the SNP. The combined P was 7.3×10^{-11} with odds ratio of 1.43 (95% CI = 1.28–1.59).

In the NCBI genome database (build 36.2), rs7639618 lies within the *LOC344875* gene. The RefSeq transcript of *LOC344875* is based on *in silico* predictions and ESTs only, so we examined the full sequence of the expressed transcript with RACE and RT-PCR. We identified a previously unknown transcript (**Supplementary Fig. 1a** online), 2,250 bp in length and with a predicted protein of 276 amino acids. Protein motif analysis programs predicted that this protein lacks a signal peptide and contains two domains homologous with the VWA domain. We named this newly identified gene *DVWA* (double von Willebrand factor A domains). Because all 17 HapMap SNPs that associated with rs7639618 with $r^2 > 0.9$ are located in and around the *DVWA* region, we surmised that *DVWA*, rather than *SH3BP5* or *CAPN7*, was likely the gene associated with osteoarthritis.

To confirm the expression and size of the *DVWA* transcript, we carried out RNA analysis and identified a band corresponding to the predicted transcript length (**Supplementary Fig. 1b**). We also examined *DVWA* expression in various human tissues using real-time PCR. The highest expression was seen in cartilage tissues from both control individuals and individuals with osteoarthritis (**Supplementary Fig. 1c**), suggesting that *DVWA* function is associated with cartilage.

To locate the functional, osteoarthritis-associated SNP, we searched for SNPs in and around all exons of *DVWA* by direct sequencing of genomic DNA from 48 individuals with knee osteoarthritis. We found 4 previously unknown SNPs in addition to 21 known SNPs in the HapMap database (**Supplementary Table 3** online). After calculating pairwise r^2 values using all 25 SNPs in the *DVWA* region (**Supplementary Fig. 2** online), we selected 7 tag SNPs with $r^2 > 0.95$. Along with the four previously genotyped SNPs, three additional SNPs (rs1287464, rs9864422 and rs11718863) were selected and genotyped. This analysis revealed that rs9864422 and rs11718863 was significantly associated with knee osteoarthritis, similar to rs7639618 (**Supplementary Table 4** online). We also checked the association of these highly associated SNPs using set C and the combined set of B and C. The association of the SNPs had similar P values and odds ratios in both set C and the combined set (**Supplementary Table 5** online).

Table 2 Association of the selected tag SNPs with knee osteoarthritis

	Case					Control						
	Genotype					Genotype					Test for allele frequency	
dbSNP ID	11	12	22	Sum	Allele 2 frequency	11	12	22	Sum	Allele 2 frequency	*P* value	Odds ratio (95% CI)
rs618762	515	101	8	624	0.094	536	78	7	621	0.074	0.077	0.77 (0.58–1.03)
rs7639618	253	293	95	641	0.377	162	327	140	629	0.483	0.000000073	1.54 (1.32–1.81)
rs353093	169	316	142	627	0.478	117	317	190	624	0.558	0.000062	1.38 (1.18–1.61)
rs826428	457	166	15	638	0.154	483	129	16	628	0.128	0.066	0.81 (0.65–1.01)
rs3773475	273	302	69	644	0.342	196	328	100	624	0.423	0.000024	1.41 (1.20–1.66)
rs11713836	317	266	49	632	0.288	255	291	77	623	0.357	0.00021	1.37 (1.16–1.63)
rs1318937	253	301	77	631	0.361	206	311	104	621	0.418	0.0033	1.27 (1.08–1.50)
rs3732728	349	251	43	643	0.262	287	283	59	629	0.319	0.0016	1.32 (1.11–1.56)
rs2291853	192	318	135	645	0.456	148	325	156	629	0.506	0.011	1.22 (1.05–1.43)
rs3773472	324	272	50	646	0.288	240	314	74	628	0.368	0.000017	1.44 (1.22–1.70)
rs3773469	228	315	102	645	0.402	163	336	126	625	0.470	0.00054	1.32 (1.13–1.54)
rs1287467	479	144	16	639	0.138	475	148	6	629	0.127	0.43	0.91 (0.73–1.15)

Population set B was genotyped. Allele 1 and allele 2 indicate the major and minor allele in the knee osteoarthritis population, respectively, and 11, 12 and 22 indicate homozygote of allele 1 and heterozygote and homozygote of allele 2, respectively. Odds ratio shown is for allele 1 versus allele 2.

Table 3 Replication of association of rs7639618 with knee osteoarthritis in Japanese and Han Chinese populations

	Case					Control						
	Genotype					Genotype					Test for allele frequency	
Population	GG	GA	AA	Sum	Allele A frequency	GG	GA	AA	Sum	Allele A frequency	*P* value	Odds ratio (95% CI)
Japanese (set C)	99	107	36	242	0.370	166	222	95	483	0.427	0.038	1.27 (1.01–1.59)
Chinese	145	187	85	417	0.428	106	192	115	413	0.511	0.00072	1.40 (1.15–1.69)

We analyzed haplotype association using the first tag-SNP set of 12 SNPs from the entire LD block and the second tag-SNP set of 7 SNPs in the *DVWA* region (**Supplementary Table 6** online). Using the first tag-SNP set, we could not find any haplotypes that had more significant effects than rs7639618. Also, we examined the additional effect of the other SNPs combined with the SNP (adding incrementally) by comparing their conditional log-likelihoods calculated by THESIAS[20], and confirmed that there was no SNP-combination haplotype more significant than rs7639618. Using the second tag SNP set, we found that *P* values of the difference between each haplotype and others were not more significant than those of rs9864422 and rs7639618. Also, there was no SNP-combination haplotype more significant than rs9864422 and rs7639618 . Therefore, we selected the most associated SNPs, rs9864422, rs11718863 and rs7639618, as candidates for the osteoarthritis-associated SNP for further functional analyses.

To identify a functional (causal) SNP, we first assessed the function of rs9864422, located in *DVWA* intron 1, using a luciferase assay, but there was no allelic difference associated with the SNP in the promoter or enhancer activity of *DVWA*. The two missense SNPs, rs11718863 (encoding Y169N) and rs7639618 (encoding C260Y), are in almost complete LD with each other, so it is not possible at this time to determine which one is the causal SNP, and they may act as a haplotype rather than a single SNP. The SNPs yielded three haplotypes; one haplotype (Tyr169-Cys260) was significantly over-represented in osteoarthritis (**Supplementary Table 7** online).

To evaluate their potential effects on DVWA function, we set out to identify binding partners of DVWA protein. Immunoprecipitation analysis of cells transfected with S-tagged *DVWA* revealed a unique band (**Fig. 1a**). Matrix-assisted laser desorption/ionization–time of flight (MALDI/TOF) mass spectrometry analysis revealed that this band corresponded to β-tubulin, and we confirmed binding between DVWA and β-tubulin by immunoprecipitation and protein blot analysis (**Fig. 1b**). Next, we assessed the binding strength between β-tubulin and DVWA isoforms. We generated S-tagged recombinant proteins corresponding to four haplotypes of the two missense SNPs (**Fig. 1c**) and carried out solid-phase binding assays. All four DVWA isoforms bound to tubulin, but binding of DVWA Tyr169-Cys260 was significantly weaker than that of the other three isoforms (**Fig. 1d**).

We have identified a previously unknown gene, *DVWA*, which is associated with knee osteoarthritis across two distinct Asian populations. DVWA protein is predicted to have two domains homologous to the VWA domain, which typically is involved in cell adhesion and protein–protein interactions. Mutations in the VWA domains of *MATN3* cause osteoarthritis[21] and osteochondrodysplasia[22]. Although most VWA-containing proteins are extracellular, some reside within the cell and have roles in transcription, DNA repair and ribosomal and membrane transport[23].

DVWA physically interacts with β-tubulin. The strength of binding is influenced by alleles of two missense SNPs, both of which are significantly associated with osteoarthritis and lie within the predicted VWA domain. The Tyr169-Cys260 isoform showed weaker binding to β-tubulin, whereas the other three isoforms showed similar degrees of interaction. Therefore, it seems that the binding is influenced by the two SNPs acting together rather than by one SNP alone. Because the Tyr169-Cys260 isoform is over-represented in osteoarthritis and shows weaker binding to β-tubulin, we infer that the interaction between DVWA and tubulin might protect joints from osteoarthritis. We could not identify a functional impact of rs9864422, but we do not rule out the possibility of its contribution to the susceptibility to osteoarthritis. It may influence the transcriptional activity of *DVWA* or nearby genes such as *CAPN7*.

Tubulin proteins and microtubules have essential roles in protein trafficking and secretion. Microtubules are also reported to regulate chondrocyte differentiation[24]. The addition of colchicine, an agent that depolymerizes microtubules, reduces the amount of collagen and glycosaminoglycan in chondrocytes[24]. Further, cartilage in a rat model of osteoarthritis shows a significant reduction in tubulin[25]. These

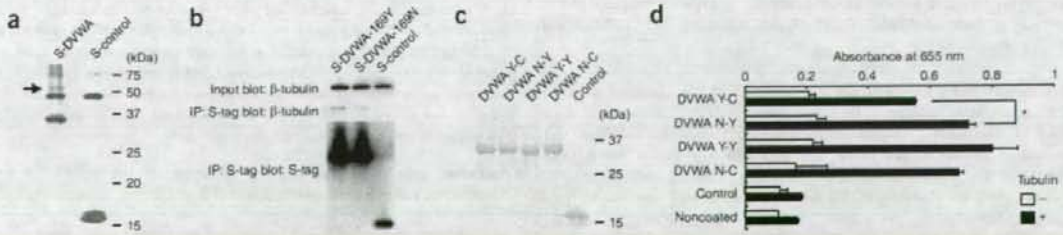

Figure 1 DVWA binds to β-tubulin. (**a**) SDS-PAGE and silver staining of samples immunoprecipitated with S-protein. Arrow indicates β-tubulin. (**b**) Confirmation of binding between DVWA and β-tubulin by protein blot. (**c**) Confirmation of DVWA recombinant proteins by SDS-PAGE. DVWA Y/N-C/Y denotes DVWA isoforms that have tyrosine (Y) or asparagine (N) at position 169, and cysteine (C) or tyrosine (Y) at position 260, respectively. (**d**) Binding strength of DVWA isoforms. Microplate wells coated with recombinant DVWA or controls were incubated with or without bovine tubulin. Data represent the mean ± s.d. in duplicate assays. The experiment was repeated three times with similar results. $^*P < 0.01$ (Student's *t*-test).

observations suggest that tubulins and microtubules might be protective factors in osteoarthritis pathogenesis. We speculate that DVWA supports intracellular transport and affects osteoarthritis susceptibility by modulating the chondrogenic function of β-tubulin. Our findings will help identify osteoarthritis pathogenesis mechanisms and aid development of improved diagnosis, treatment and prevention methods.

METHODS

Subjects. We recruited individuals with knee osteoarthritis and control individuals in sets A and B through several medical institutes in Japan, as previously described[11]. All individuals in the osteoarthritis populations were over 40 years of age. Osteoarthritis was diagnosed on the basis of clinical and radiographic findings using previously described criteria[11,26,27]. Knee osteoarthritis populations include individuals with joint-space-narrowing grade 2 or higher[26]. For set C, we recruited population-based cohorts from inhabitants of Odai and Minami-ise town (previously Miyagawa village and Nansei town, respectively[10]) in the Mie prefecture in Japan. Each subject was classified into the knee osteoarthritis or control group on the basis of radiographic findings, as previously described[10]. The Han Chinese knee osteoarthritis and control populations were recruited as described previously[11,12] from the Center for Diagnosis and Treatment of Joint Disease and the Center of Physical Examination at Drum Tower Hospital. Clinical parameters for the populations in this study are shown in **Supplementary Table 8** online. There was no significant difference in mean age, BMI and sex distribution for the genotypes of rs7639618 among the Japanese and Chinese populations studied (**Supplementary Table 1**). We obtained written informed consent from each subject as approved by the ethical committees of the SNP Research Center at RIKEN, the Medical School of Nanjing University and participating clinical institutes.

Genotyping of SNPs. We extracted genomic DNA from peripheral blood leukocytes of affected individuals and controls using standard protocols. We genotyped SNPs using the multiplex PCR–based Invader assay[28] (Third Wave Technologies) or TaqMan SNP genotyping assays (Applied Biosystems), or by direct sequencing of PCR products using ABI 3700 DNA analyzers (Applied Biosystems), according to the manufacturers' protocols. We checked the quality of genotyping data of the initial genome-wide screening and the replication study, and omitted SNPs whose genotyping success rate was lower than 90%, or whose Hardy-Weinberg equilibrium P value of the control population was lower than 0.01.

Statistical analysis. We estimated haplotype frequencies using the EM algorithm. We carried out statistical analyses for the association, haplotype frequencies and Hardy-Weinberg equilibrium and for calculation of linkage disequilibrium coefficients (D' and r^2) using Haploview software 3.32 (ref. 29) and Microsoft Excel. We selected tag SNPs using Haploview with a pairwise tagging mode. We analyzed the effect of each haplotype to the disease using THESIAS[30]. Also, we analyzed effect of SNP-combination haplotypes by adding SNPs incrementally (in a stepwise manner) and by comparing their conditional log-likelihoods calculated by THESIAS with Akaike criterion (AIC).

Cell culture and RNA extraction. We cultured HEK293, chondrogenic HCS-2/8 and OUMS-27 cells in DMEM containing 10% FBS (FBS) at 37 °C under 5% CO_2. Normal human articular chondrocytes (NHAC-kn; Cambrex) were purchased and maintained in the supplied medium of the kit. We extracted mRNA for RACE, RT-PCR and RNA blot analysis from cultured cells using the FastTrack 2.0 Kit (Invitrogen). Total RNA from cultured cells was extracted using Isogen (Nippongene) and SV Total RNA Isolation System (Promega).

We obtained knee osteoarthritis cartilage from total knee arthroplasties (7 samples). Normal cartilage was obtained from the femoral heads of control individuals during surgery for femoral neck fractures (8 samples). None of the control individuals had a clinical history or radiographic signs of osteoarthritis. We extracted total RNAs from cartilage using the RNeasy Lipid Tissue Kit (Qiagen).

RACE, RT-PCR and real-time PCR. We carried out 5′ and 3′ RACE using the SMART RACE cDNA Amplification Kit (Clontech) according to the manufacturer's protocol. We used mRNA (1 μg) of NHAC to produce the RACE template. Multiple Tissue cDNA Panels (Clontech) were used to examine all tissues other than cartilage. cDNA from cartilage and cell lines was synthesized for RT-PCR and real-time PCR using Multiscribe reverse transcriptase and an oligo-dT primer (Applied Biosystems). We carried out quantitative real-time PCR using an ABI PRISM 7700 sequence detector with the Quantitect SYBR Green PCR Kit (Qiagen) in accordance with the manufacturers' instructions.

RNA blotting. We cloned the cDNA fragment corresponding to nucleotides 510–1,517 of *DVWA* into the pCR2.1TOPO vector (Invitrogen). The DIG-labeled probe was synthesized from the constructed vector using the DIG RNA Labeling Kit (Roche). We used 4 μg of NHAC, HCS-2/8 and OUMS-27 mRNA for gel electorophoresis. Transfer, hybridization and detection were done using the DIG Easy Hyb and DIG Wash and Block Buffer set (Roche) according to the manufacturer's instructions.

Luciferase assay. We determined the core promoter region of *DVWA* and cloned a native *DVWA* promoter (nucleotide −342 to +34; the number is from the transcription start site of *DVWA*) into pGL3-basic vector (Promega), which contained the firefly luciferase gene (*Luc*). We also cloned 675-bp fragments from the genomic sequence around rs9864422 (rs9864422 fragment) that contained either allele of the SNP. Using the native *DVWA* promoter, we constructed two kinds of vectors for each allele of rs9864422 that contained the rs9864422 fragments 5′ or 3′ to the luciferase gene: (from upstream) *DVWA* promoter-rs9864422 fragment-Luc and *DVWA* promoter-Luc- rs9864422 fragment. We constructed similar vectors containing the SV40 promoter instead of the *DVWA* promoter. We transfected cells (5×10^4) with 0.4 μg of the constructed pGL3 vectors and 4 ng of the pRL-TK vector as an internal control, using TransIT-293 (for HEK293) or TransIT-LT1 (for other cell lines) reagent (Mirus). After 48 h, we collected the cells and measured luciferase activity using the PicaGene Dual Sea Pansy system (Toyo Ink).

Immunoprecipitation. The entire coding sequence of *DVWA* was cloned into the pTriEx4 vector (Novagen), which expresses N-terminal S-tagged DVWA in mammalian cells. The vector or pTriEx4 alone (which expresses S-tagged artificial control protein) was transiently transfected into HCS-2/8 or HEK293 cells. Immunoprecipitation was done on cell lysates using S-protein agarose (Novagen) according to the manufacturer's instructions. Following SDS-PAGE, target protein bands were analyzed by MALDI/TOF mass spectrometry at APRO Life Science, or by protein blotting using antibody to β-tubulin (Santa Cruz) and S-protein-HRP (Novagen).

Recombinant protein and solid-phase binding assay. Rosetta (DE3) pLacI (Novagen) was transformed with pTriEx4-*DVWA* and cultured in the Overnight Express Autoinduction System (Novagen). We extracted recombinant DVWA protein using BugBuster Protein Extraction Reagent (Novagen), and refolded it from an insoluble fraction using Protein Refolding Kit (Novagen). Maxisorp ELISA plate (Nunc) wells were coated with 100 μl of 50 μg/ml recombinant S-tagged DVWA protein in 50 mM $NaHCO_3$ buffer (pH 9.6) at 4 °C overnight. Wells were blocked with 100 μl of 5% BSA in PBS; 5 μg of bovine tubulin (Cytoskeleton) was added in a total volume of 100 μl of 5% BSA in PBS and incubated overnight at 4 °C. Wells were washed three times with 20 mM Tris-HCl (pH 7.5), 137 mM NaCl and 0.05% Tween 20 (TBST) and incubated with β-tubulin-HRP antibody (Santa Cruz) for one hour. After washing five times with TBST, we assayed bound tubulin using the TMB Peroxidase EIA Substrate Kit (Biorad).

Accession codes. DNA Data Bank of Japan: *DVWA* mRNA sequence, AB299979. GenBank: *LOC344875*, XM_497913.

Note: Supplementary information is available on the Nature Genetics website.

ACKNOWLEDGMENTS

We thank all individuals who participated in the study. We also thank S. Yamamoto, A. Fukuda, A. Kawakami, T. Kubo, Y. Takatori, S. Saito, A. Mabuchi, K. Nakamura and I. Kou for help with the research, and Y. Takanashi and T. Kusadokoro for excellent technical assistance.

AUTHOR CONTRIBUTIONS

Y.M. carried out the Japanese knee osteoarthritis association study and *in vitro* functional assay together with M.N. and prepared the manuscript. D.S. carried out the Chinese association study. K.O., A.S., A.K., A.U., N.E., Y.N. and T.Tanaka managed DNA sample and clinical information and contributed data interpretation. A.T. and T.Tsunoda helped with statistic analysis. Q.J. managed the Chinese association study. S.I. planned and supervised the whole project.

Published online at http://www.nature.com/naturegenetics/
Reprints and permissions information is available online at http://npg.nature.com/reprintsandpermissions/

1. Ikegawa, S. New gene associations in osteoarthritis: what do they provide, and where are we going? *Curr. Opin. Rheumatol.* **19**, 429–434 (2007).
2. Spector, T.D. & MacGregor, A.J. Risk factors for osteoarthritis: genetics. *Osteoarthritis Cartilage* (12 Suppl. A), S39–44 (2004).
3. Celikel, R. *et al.* Crystal structure of the von Willebrand factor A1 domain in complex with the function blocking NMC-4 Fab. *Nat. Struct. Biol.* **5**, 189–194 (1998).
4. Dieppe, P.A. & Lohmander, L.S. Pathogenesis and management of pain in osteoarthritis. *Lancet* **365**, 965–973 (2005).
5. Hunter, D.J. & Felson, D.T. Osteoarthritis. *Br. Med. J.* **332**, 639–642 (2006).
6. Pollard, B. & Johnston, M. The assessment of disability associated with osteoarthritis. *Curr. Opin. Rheumatol.* **18**, 531–536 (2006).
7. Gupta, S., Hawker, G.A., Laporte, A., Croxford, R. & Coyte, P.C. The economic burden of disabling hip and knee osteoarthritis (OA) from the perspective of individuals living with this condition. *Rheumatology (Oxford)* **44**, 1531–1537 (2005).
8. Spector, T.D., Cicuttini, F., Baker, J., Loughlin, J. & Hart, D. Genetic influences on osteoarthritis in women: a twin study. *Br. Med. J.* **312**, 940–943 (1996).
9. Loughlin, J. *et al.* Functional variants within the secreted frizzled-related protein 3 gene are associated with hip osteoarthritis in females. *Proc. Natl. Acad. Sci. USA* **101**, 9757–9762 (2004).
10. Kizawa, H. *et al.* An aspartic acid repeat polymorphism in asporin inhibits chondrogenesis and increases susceptibility to osteoarthritis. *Nat. Genet.* **37**, 138–144 (2005).
11. Miyamoto, Y. *et al.* A functional polymorphism in the 5′ UTR of GDF5 is associated with susceptibility to osteoarthritis. *Nat. Genet.* **39**, 529–533 (2007).
12. Jiang, Q. *et al.* Replication of the association of the aspartic acid repeat polymorphism in the asporin gene with knee osteoarthritis susceptibility in Han Chinese. *J. Hum. Genet.* **51**, 1068–1072 (2006).
13. Valdes, A.M. *et al.* Sex and ethnic differences in the association of ASPN, CALM1, COL2A1, COMP, and FRZB with genetic susceptibility to osteoarthritis of the knee. *Arthritis Rheum.* **56**, 137–146 (2007).
14. Ozaki, K. *et al.* Functional SNPs in the lymphotoxin-alpha gene that are associated with susceptibility to myocardial infarction. *Nat. Genet.* **32**, 650–654 (2002).
15. Mototani, H. *et al.* A functional single nucleotide polymorphism in the core promoter region of CALM1 is associated with hip osteoarthritis in Japanese. *Hum. Mol. Genet.* **14**, 1009–1017 (2005).
16. Kubo, M. *et al.* A nonsynonymous SNP in PRKCH (protein kinase C eta) increases the risk of cerebral infarction. *Nat. Genet.* **39**, 212–217 (2007).
17. Haga, H., Yamada, R., Ohnishi, Y., Nakamura, Y. & Tanaka, T. Gene-based SNP discovery as part of the Japanese Millennium Genome Project: identification of 190,562 genetic variations in the human genome. Single-nucleotide polymorphism. *J. Hum. Genet.* **47**, 605–610 (2002).
18. Pritchard, J.K. & Rosenberg, N.A. Use of unlinked genetic markers to detect population stratification in association studies. *Am. J. Hum. Genet.* **65**, 220–228 (1999).
19. Freedman, M.L. *et al.* Assessing the impact of population stratification on genetic association studies. *Nat. Genet.* **36**, 388–393 (2004).
20. Tregouet, D.A. & Garelle, V. A new JAVA interface implementation of THESIAS: testing haplotype effects in association studies. *Bioinformatics* **23**, 1038–1039 (2007).
21. Stefansson, S.E. *et al.* Genomewide scan for hand osteoarthritis: a novel mutation in matrilin-3. *Am. J. Hum. Genet.* **72**, 1448–1459 (2003).
22. Mabuchi, A. *et al.* Novel and recurrent mutations clustered in the von Willebrand factor A domain of MATN3 in multiple epiphyseal dysplasia. *Hum. Mutat.* **24**, 439–440 (2004).
23. Whittaker, C.A. & Hynes, R.O. Distribution and evolution of von Willebrand/integrin A domains: widely dispersed domains with roles in cell adhesion and elsewhere. *Mol. Biol. Cell* **13**, 3369–3387 (2002).
24. Farquharson, C., Lester, D., Seawright, E., Jefferies, D. & Houston, B. Microtubules are potential regulators of growth-plate chondrocyte differentiation and hypertrophy. *Bone* **25**, 405–412 (1999).
25. Capin-Gutierrez, N., Talamas-Rohana, P., Gonzalez-Robles, A., Lavalle-Montalvo, C. & Kouri, J.B. Cytoskeleton disruption in chondrocytes from a rat osteoarthrosic (OA)-induced model: its potential role in OA pathogenesis. *Histol. Histopathol.* **19**, 1125–1132 (2004).
26. Ikeda, T. *et al.* Identification of sequence polymorphisms in two sulfation-related genes, PAPSS2 and SLC26A2, and an association analysis with knee osteoarthritis. *J. Hum. Genet.* **46**, 538–543 (2001).
27. Mabuchi, A. *et al.* Identification of sequence polymorphisms of the COMP (cartilage oligomeric matrix protein) gene and association study in osteoarthrosis of the knee and hip joints. *J. Hum. Genet.* **46**, 456–462 (2001).
28. Ohnishi, Y. *et al.* A high-throughput SNP typing system for genome-wide association studies. *J. Hum. Genet.* **46**, 471–477 (2001).
29. Barrett, J.C., Fry, B., Maller, J. & Daly, M.J. Haploview: analysis and visualization of LD and haplotype maps. *Bioinformatics* **21**, 263–265 (2005).